Discover Sustainability

Discover

Brief Communication

Maximizing the output power for electric vehicles charging station powered by a wind energy conversion system using tip speed ratio

Amro A. Kawashty[1] · Sameh O. Abdellatif[2] · Gamal A. Ebrahim[3] · Hani A. Ghali[2]

Received: 17 June 2023 / Accepted: 5 September 2023
Published online: 26 September 2023

Abstract
This study investigates the influence of tip speed ratio (TSR) as maximum power point tracking (MPPT) technique on energy conversion for wind-powered electric vehicles (EVs) charging stations. The data for 14 different models of (EVs) as well as the energy demand profile for El Sherouk city in new Cairo, Egypt, is used in the study. Those vehicles represent the models that are most likely to be used according to the nature of the Egyptian market from economic and technological concerns. This includes range, battery capacity, battery technology and charging methods. charging can be in the form of fast DC, three phases which are suitable for commercial charging stations or a single phase charging suitable for residential use. A simulation is done using MATLAB/Simulink for a wind turbine Permanent Magnet Synchronous Generator (PMSG) system including TSR MPPT algorithm. The energy output is compared with and without implementing the MPPT algorithms to measure the difference in energy. The system simulation optimized by the TSR MPPT algorithm shows an increase in the energy yield by 41.68%. The economic analysis showed a 30% reduction in the levelized cost of energy while utilizing the TSR concerning a bare system without an MPPT algorithm.

Keywords Wind energy conversion system (WECS) · Maximum power point tracking (MPPT) · Tip speed ratio (TSR) · Electric vehicles (EVs) · Techno-economic analysis

List of symbols

β	The pitch angle (Read)
λ	The turbine tip speed ratio (1)
ω_m	The turbine's rotational speed (Rad/sec.)
ω_{opt}	The turbine's optimum rotational speed (Rad/sec.)
τ	The response time (Sec.)
$Cp(\lambda, \beta)$	The power coefficient (1)
D	Initial duty cycle (1)
d	Optimized duty cycle (1)
Δd	Duty cycle step size (1)
f	The Viscos friction (N m sec)
J	The Combined inertia (Kg m^2)

✉ Sameh O. Abdellatif, sameh.osama@bue.edu.eg | [1]Faculty of Engineering FabLab in the Center for Emerging Learning Technology (CELT), Renewable Energy Program, The British University in Egypt (BUE), Suez Rd, El Sherouk City, Cairo 11837, Cairo, Egypt. [2]The Electrical Engineering Department, Faculty of Engineering and FabLab, Centre for Emerging Learning Technologies (CELT), The British University in Egypt (BUE), Elshrouk City, Cairo, Egypt. [3]Computer and Systems Engineering Department, Faculty of Engineering, Ain Shams University, Cairo 11517, Egypt.

K	A constant dependent on the characteristics of each specific turbine (1)
K_i	The integral gain (1)
K_p	The proportional gain (1)
$LCOE$	The levelized cost of energy ($/kW h)
P_m	The turbine outputs mechanical power (kW)
R	The turbine radius (m)
T_m	The turbine torque (N m)
T_e	The electromagnetic torque (N m)
V_{dc}	Output DC voltage from the wind turbine (V)
EVs	Electric vehicles
DPC	Direct power control
IRR	The interest rate of return
IPC	Indirect power control
MPPT	Maximum power point
O&M	Operation and maintenance
PMSG	Permanent Magnet Synchronous Generator
WECS	Wind energy conversion systems

1 Introduction

Climate change has recently been a significant concern due to its negative impact on the environment [1–3]. The leading cause of climate change is the annual increase in energy demand as technology develops [4, 5]. The automotive industry is one of the highest developed, energy-consuming, and air-polluting industries because of fossil fuel combustion [6]. As a result, for the past decade, the automotive industry is experiencing an increase in electric vehicles (EVs) share of the automotive market because it produces zero emissions [7–9], with considering the carbon footprint of EV manufacturing [10]. As the number of EVs increases, the energy demand on the grid increases, negatively impacting the function of the grid [11–13]. Moreover, there is no environmental benefit from charging EVs using a fossil-fueled grid. On the contrary, this may increase emissions because of energy losses and low energy conversion efficiency [14].

The solution to this problem is a clean, optimized, highly efficient energy alternative for EV charging stations [15–17]. Many kinds of research have attempted to design EV charging stations taking into consideration renewable energy utilization from different points of view [15, 18, 19]. One of the effective ways to increase the energy conversion efficiency and thus increase the output energy is utilizing maximum power point tracking (MPPT) algorithms that ensure the system is operating at the maximum operating point [20, 21]. To do so, some studies have investigated the effect of implementing different MPPT techniques, especially those integrated into wind energy conversion systems (WECS) [20, 22]. MPPT algorithms are classified into indirect power control (IPC) and direct power control (DPC) [23]. The IPC consists of tip speed ratio (TSR), optimum torque control, and power signal feedback, which depends mainly on measuring wind speed as an input variable for the algorithm to reach the maximum operating point corresponding to each wind speed [24]. On the other hand, DPC algorithms are an iterative approach that uses perturb parameters like turbine speed, torque, current, and voltage to identify the optimum duty cycle to be implemented by the power electronic circuit in the power converter to maintain operation at maximum power point under the dynamic nature of the wind [25].

In wind energy conversion systems, the TSR is often used as a means of MPPT [26, 27]. The TSR is the ratio of the speed of the wind turbine blade tip to the speed of the wind passing over the blade. MPPT is a crucial aspect of wind energy systems because it ensures that the wind turbine operates at its maximum efficiency and extracts the maximum available kinetic energy from the wind. By constantly adjusting the TSR, the wind turbine can maintain an optimum operating point, maximizing power extraction from the wind [26, 27]. This approach is widely used in modern wind turbine control strategies to ensure efficient and effective operation. It is important to note that while TSR-based MPPT effectively extracts maximum power under normal operating conditions, there may be limitations in extreme wind conditions where the turbine needs to enter a protection mode to prevent damage. In such cases, additional control strategies may be employed to safeguard the wind turbine's integrity [28]. Through the reported literature, we could not catch any study that quantitively the impact of the MPPT techniques, especially in WECS, on the techno-economic feasibility of a specific system. Consequently, we consider such techno-economic investigation as a literature gap.

This study presents a comprehensive analysis of maximizing the output power for an Electric Vehicle charging station powered by a wind energy conversion system using TSR with a techno-economic approach. The research focuses on implementing TSR-based MPPT strategy in the wind turbine to achieve optimal power extraction efficiency. A thorough techno-economic analysis considers factors such as wind resource assessment, turbine size, transmission losses, distribution losses, and grid integration. The objective is to determine the feasibility and economic viability of integrating a wind energy conversion system to power EV charging station, ensuring maximum power output while minimizing operational costs. The findings provide insights into the technical and economic considerations for successfully implementing this renewable energy-integrated charging infrastructure.

The paper is layout in five sections, rather than the introduction section. Section two illustrate the inputs related to the location data, wind profile and EV database. In section three, the energy budget, in terms of supply and demand is discussed. Followed by a detailed description about the TSR algorithm. Section five represents both technical and economic results, while the manuscript is terminated by conclusions.

2 Location data and EVs specification

2.1 Location

Recently Egyptian automotive market has been transitioning into EVs and plug-in hybrids according to the 2030 automotive market vision [29], increasing the energy demand from the grid. Because of that, an innovative and efficient energy alternative should be considered. This study takes place in El Sherouk City in New Cairo, Egypt. The wind data used in this study is from Cairo international airport weather station (see Fig. 1) according to the weather underground website with twice readings per hour for the year 2020 [30] (see the wind profile in Fig. 1; the wind rose in Fig. 2. and wind Weibull distribution in Fig. 3.).

2.2 Electric vehicles specifications and charging behavior in Egypt

In the current study, the EV station was considered the electric load powered by the wind energy conversion system. The data of 14 EVs from the Egyptian market, including battery capacity in KW. h, energy consumption W h/Km, and their charging behavior (as shown in Fig. 4.) is collected to be used in the study, as shown in Table 1 [15, 18]. These data were used to calculate the total daily energy consumption, which is 3400 kW h/day. As demonstrated later, this value is utilized with the wind characteristics in sizing the required wind turbine to be used in El Sherouk city in new Cairo, Egypt, for an EVs charging station.

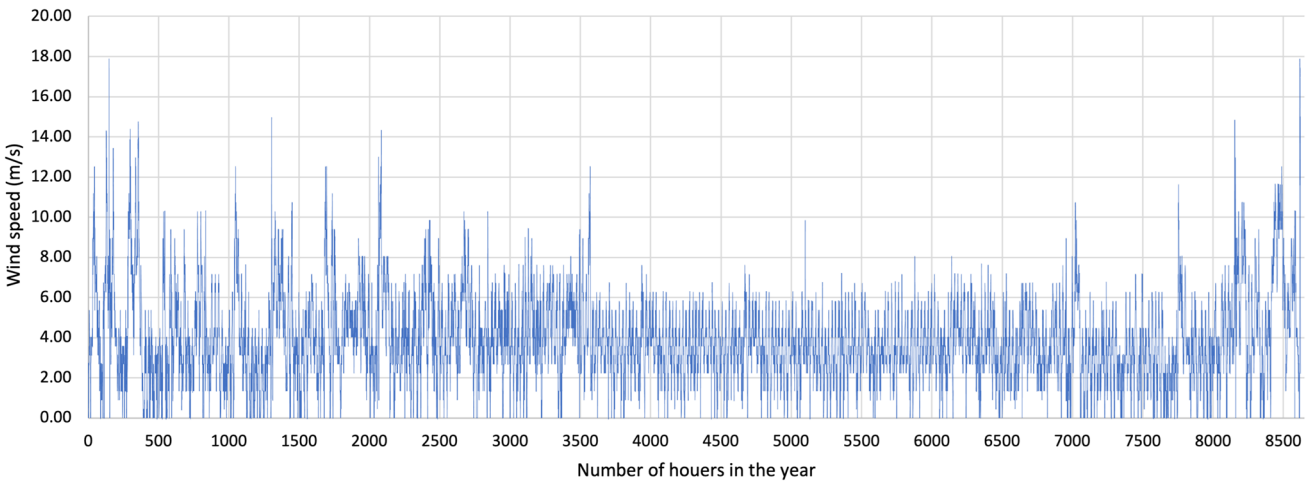

Fig. 1 Wind profile in El-Shorok city

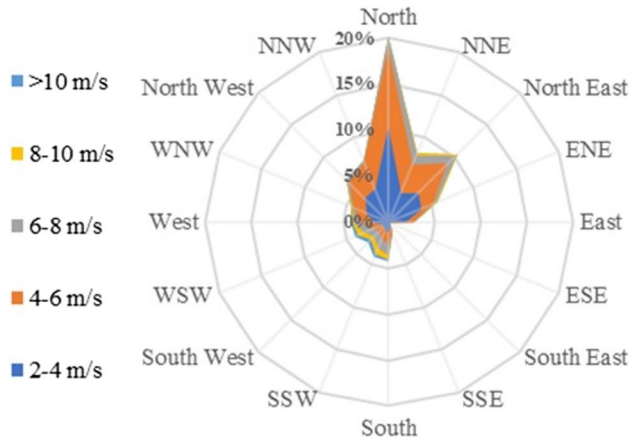

Fig. 2 El Sherouk city wind rose

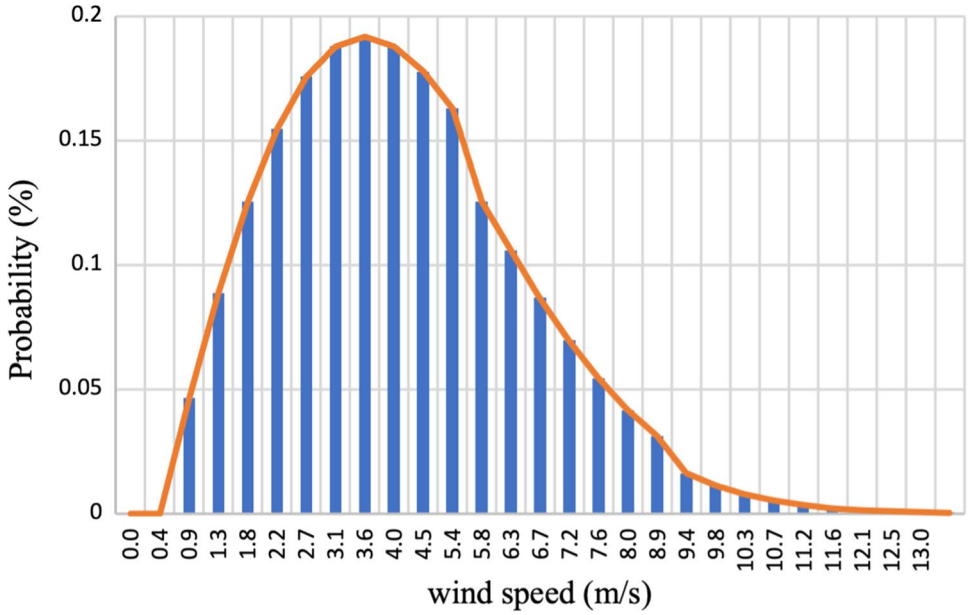

Fig. 3 El Sherouk city wind Weibull distribution

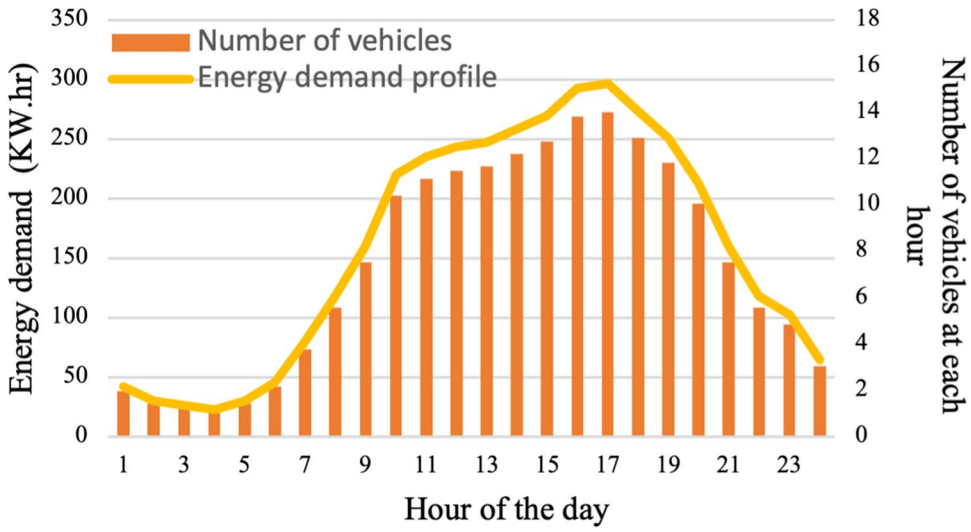

Fig. 4 EVs load profile and charging behavior in the Egyptian automotive market

Table 1 Electric vehicles selection data

Car type	Battery capacity (kW h)	Energy consumption W h/km
Mercedes EQC 400 (4 matic) 2019	85.0	224
2016 CHEVROLET SPARK	21.6	130
skoda-citigo-e-iv 2020	36.8	162
Fiat 500 2018	42.0	170
Nissan leaf 2013	24.0	170
e-Golf 2015	24.0	158
SEAT-el-Born 2019 (VWid3)	61.5	171
2012 Mitsubishi i-MiEV	16.0	171
2015 Kia Soul EV	27.0	180
2014 BMW i3	21.6	170
Toyota rav4 (2014)	41.8	252.17
Honda Clarity 2020 [PHEV}	25.5	46.6
2014 Tesla Model S	85.0	206
Peugeot ion 2011	16.3	171

3 Matching supply and demand energy

The process of sizing any power plant is dependent on the energy demand, and so is the EVs charging station scenario, which needs a 45 m radius 3.5 MW wind turbine as a minimum that generates 1640 MWh to cover the 1241 MWh EVs energy demand with excess electricity 32% (as shown in Fig. 5) to compensate for energy losses and the growth in EVs market in Egypt. Another point of view should be considered in sizing any WECS, which is the effect of implementing the MPPT algorithm, and this is the focus of this study.

3.1 Wind turbine modeling

Wind turbines are devices that convert wind Kinetic energy to mechanical energy. The output mechanical power produced by a turbine drives an electric generator [21, 25]. For a variable-speed wind turbine, the mechanical output power and torque could be calculated from the following formulas, which can be used to construct the $P_m - \omega_m$ characteristic curves shown in Fig. 6, while the electrical performance of the turbine is demonstrated in terms of the $P_m - V_{dc}$ characteristic curves shown in Fig. 7, see equations (1) to (3).

$$P_m = \mathrm{K} \cdot \omega_{m\bullet}^3 Cp(\lambda, \beta) \tag{1}$$

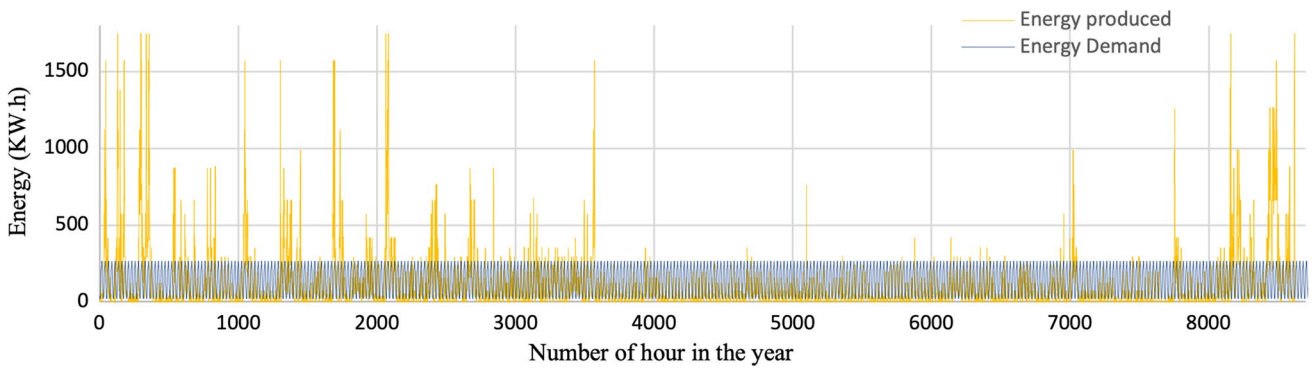

Fig. 5 Supply–demand energy matching

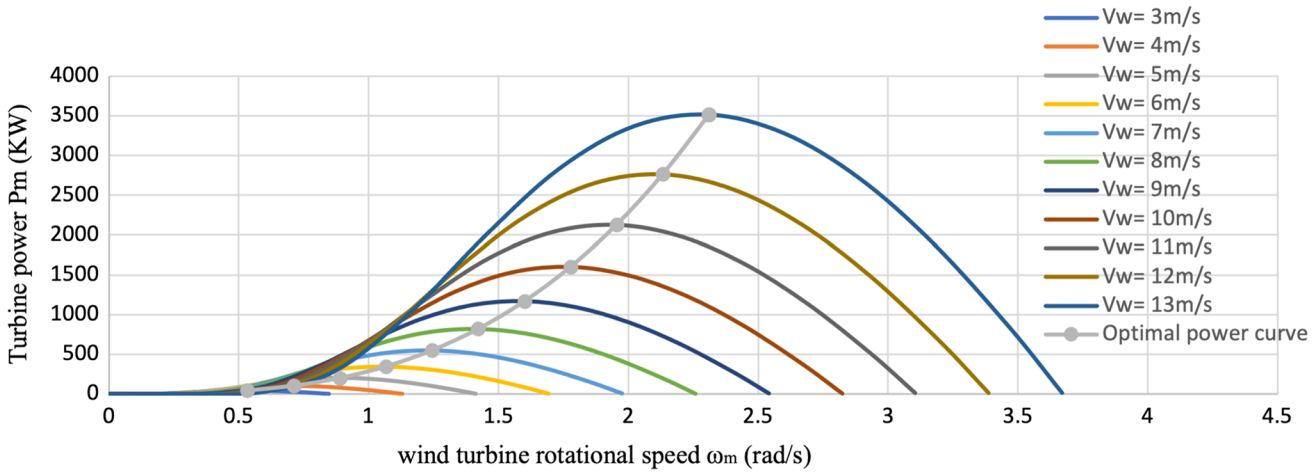

Fig. 6 Wind turbine optimum power curve

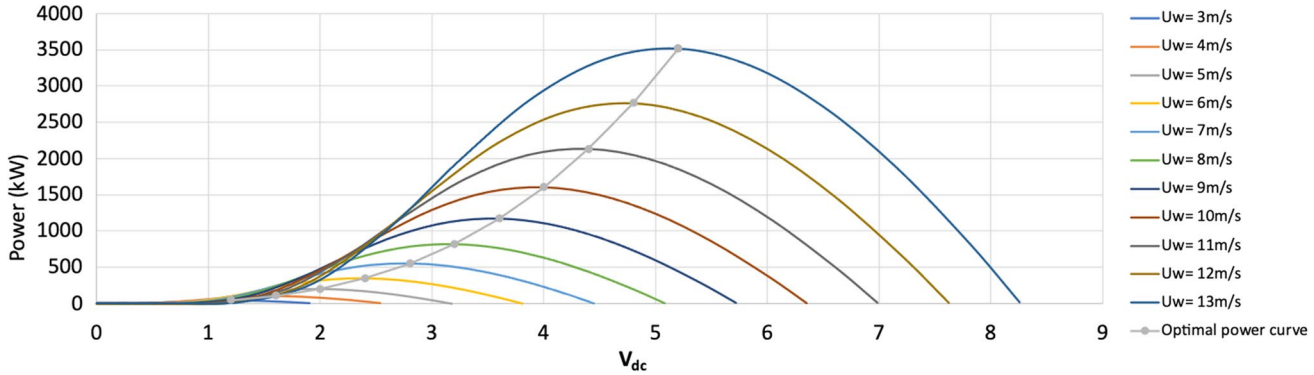

Fig. 7 Wind turbine $P_m - V_{dc}$ characteristic curves

$$T_m = \mathrm{K} \cdot \omega_m^2 \tag{2}$$

$$\mathrm{K} = \frac{1}{2}\rho \cdot \pi \cdot \frac{R^5}{\lambda^3} \tag{3}$$

P_m is the turbine output mechanical power, ω_m is the turbine rotational speed, K is a constant dependent on the characteristics of each specific turbine, T_m is the turbine torque, R is the turbine radius, λ is the turbine tip speed ratio, β is the pitch angle and $Cp(\lambda, \beta)$ is the power coefficient it is expressed by different models [31] and the following formula will be used, equations (4) to (6).

$$C_p(\lambda, \beta) = \frac{1}{2}\left(116\frac{1}{\lambda_i} - 0.4\beta - 5\right)\mathrm{e}^{\frac{-21}{\lambda i}} \tag{4}$$

$$\frac{1}{\lambda_i} = \frac{1}{\lambda + 0.08\beta} - \frac{0.035}{1 + \beta^3} \tag{5}$$

$$\lambda = \frac{\omega_m R}{V_w} \tag{6}$$

$C_p(\lambda, \beta)$ is at maximum value if and only if the $\beta = 0, \lambda = \lambda_{opt}$ as shown in Fig. 8. According to Eq. (1), P_m is maximum in case the turbine is rotating at the optimum speed according to the input wind speed. The rotational speed of wind turbines is

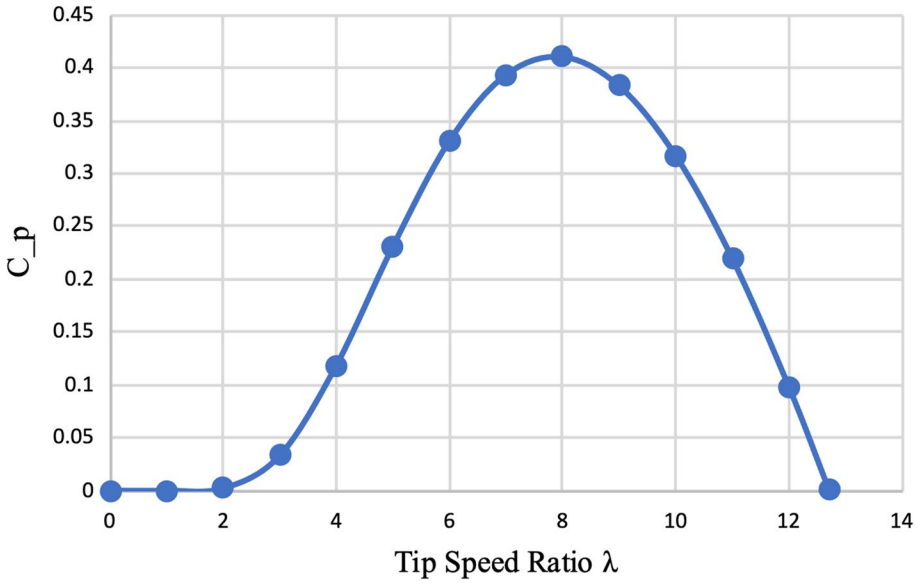

Fig. 8 Power coefficient and tip speed ratio relationship

obtained by the mathematical relation between turbine mechanical torque, generator electromagnetic torque, and turbine inertia, as shown in the following equation (7).

$$J \cdot \frac{d\omega_m}{dt} = T_e - T_m - f.\omega_m \tag{7}$$

4 TSR MPPT algorithm simulation

In the TSR method, the main system objective to extract the maximum power is to keep the TSR value at the optimum value according to the input wind speed. To do so, wind speed and generator speed are measured. Then the MPPT controller identifies the optimum rotational speed by using the optimum power curve of the turbine. Finally, the controller compares the optimum wind speed with the actual rotational speed, and the power converter uses this difference to regulate the generator speed (see the TSR schematic in Fig. 9, with the algorithm flowchart in Fig. 10, and the Simulink entire model in Fig. 11) [32]. K_i and K_p are the integral and proportional gains expressed by the following formulas [33], equations (8), and (9).

$$K_i = \frac{f}{\tau} \tag{8}$$

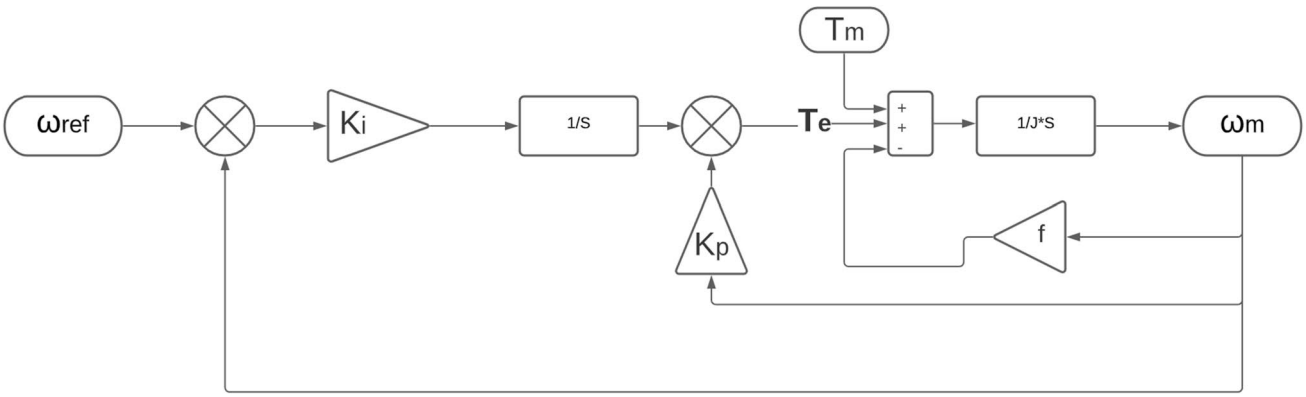

Fig. 9 TSR MPPT algorithm control block diagram

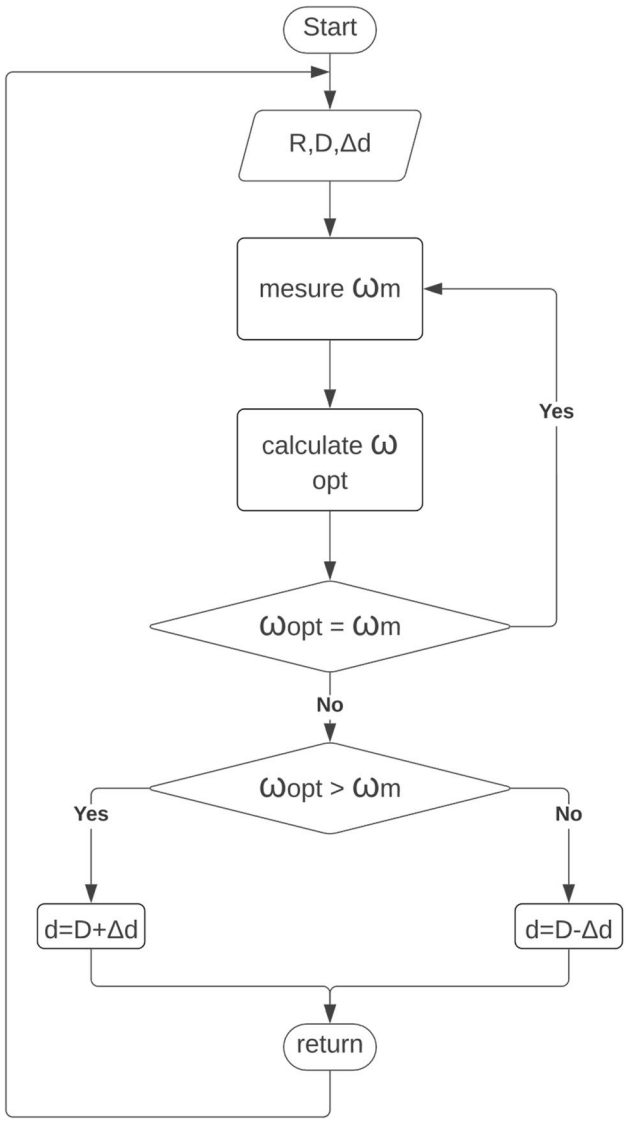

Fig. 10 TSR MPPT algorithm flowchart algorthim

$$K_p = \frac{J}{\tau} \tag{9}$$

where f is the viscous friction, J is the combined inertia, and τ is the response time.

Following the demonstrations in Figs. 9, and 10, the TSR MPPT algorithm is directly dependent on wind speed characterized by its dynamic nature. To get the most benefit using this MPPT method, the used controller should maintain steady-state error and offer high stability when reaching the peak value, which is the optimal power curve. The PI controller fulfills those requirements considering the reduction in cost and complexity of implementation compared to the PID controller, which could be used in this application. In other words, the PID controller offers outstanding performance in most applications, precisely the TSR MPPT technique. However, it is complex and costs more, making the slight performance improvement unfeasible.

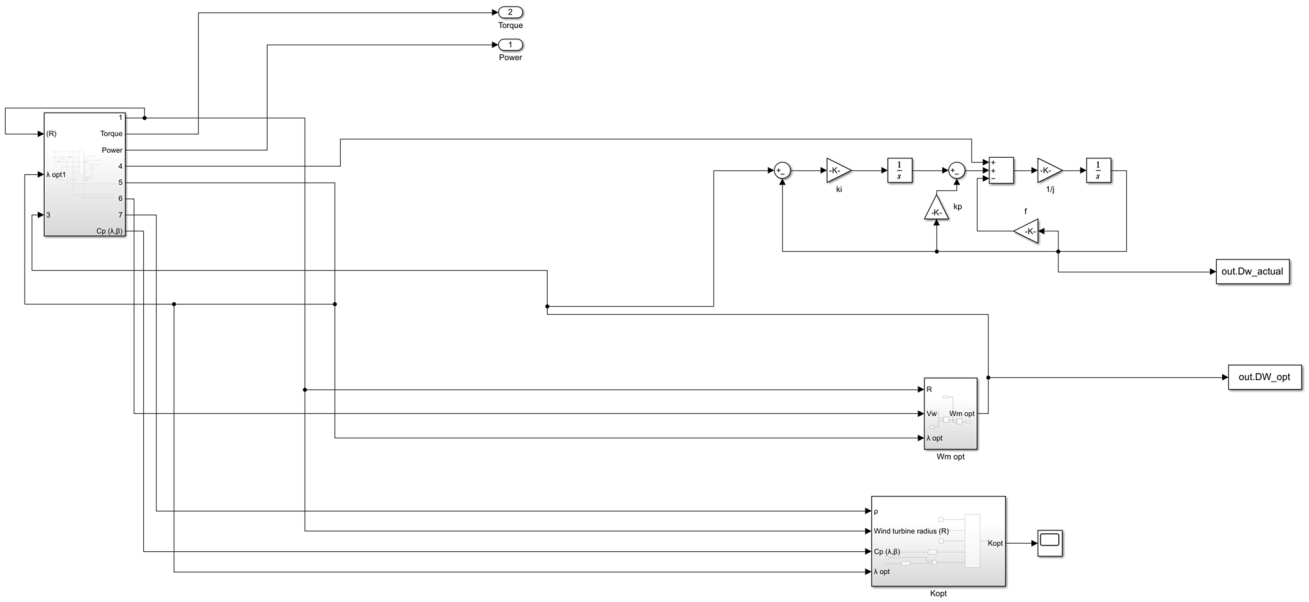

Fig. 11 Simulink block diagram

5 Results and discussion

5.1 TSR simulation results

TSR simulation was implemented according to the turbine sizing for the EVs data listed in Table 1, applying the schematic shown in Fig. 9 and the data listed in Table 2. To test the utility of the TSR as an MPPT method used in WECS, the system under test is investigated in terms of extracted power against a bare system, i.e., without any MPPT. Figure 12 shows the difference in energy generation with TSR and without, using a sample of the wind data to prove the concept. Utilizing TSR as an MPPT algorithm resulted in a 41.68% increase in the energy yield, making the system future-proof and offering the convenience of expanding the charging station as the EV population increases. Moreover, improving the energy yield provides the privilege of reducing the turbine size as a second option. The system's technical outputs are listed in Table 3. It is worth highlighting that the wind turbine dimensions, leading to a 3.5 MW system, were chosen to meet the load requirements. Scaling down to a lower standard would result in a shortage in power generation. Alternatively, the selected model recorded a 32% excess energy production under the bare system and 87% excess energy production under the TSR-added MPPT algorithm, cf. Table 3. We consider such excess energy as part of the system's added value. On the one hand, this excess energy can be directed to the grid. On the other hand, it enables the expandability of the station, where a higher density of EVs and charging points can be added.

5.2 Economic and environmental analysis

As mentioned earlier, the impact of using MPPT in WECS is addressed in generating more power by optimizing the operation under various wind speeds. Accordingly, such impact should have a direct influence on the system's economics, as well as the environmental aspects. In this section, we attempt to estimate the system economics while still

Table 2 Wind turbine system parameters

Parameter	Value
Wind turbine radius	R = 45 m
Viscous friction	f = 0.0022 N m s
Combined inertia	J = 1000 kg m^2
Response time	τ = 0.02 s

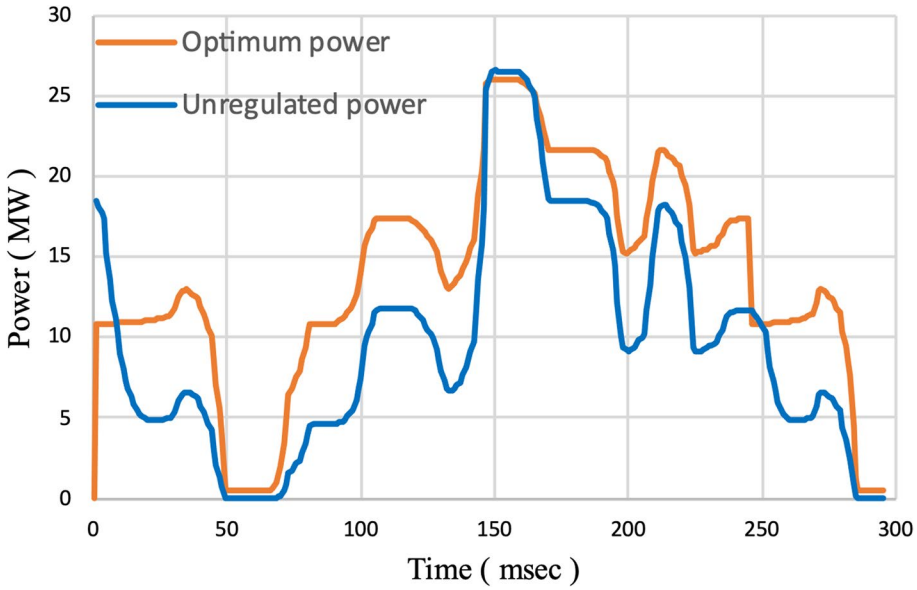

Fig. 12 The extracted power with and without TSR

Table 3 Wind turbine system techno-economic output parameters

Economic analysis for wind turbine		
3.5 MW bare WECS cost	5,253,500	$
3.5 MW bare WECS cost	5,256,753	$
Operation and maintenance (bare system)	40	$/kW/yr
Operation and maintenance for TSR	6	$/kW/yr
Inflation rate	5	%
Annual energy production (bare system)	1640	MW.h/yr
Annual energy production (with TSR)	2323.552	MW.h/yr
Annual load requirement	1241	MW.h/yr
Excess energy ratio under bare system	1.321514907	
Excess energy ratio with TSR	1.872322321	

Table 4 Wind turbine system with and without TSR economic output parameters

	Bare system	System with TSR
Capital Cost in $	5,253,500	5,256,753
O&M in $/kW h/year	40	46
Annual Energy production in MW	1640	2323.552
LCOE in $/kW.h	0.318	0.225
Payback period. In years	6.5	5
IRR in %	15.2	16.3

referring to the system without MPPT as the bare system. The added cost, either as capital or operation and maintenance costs for TSR, are listed in Table 4. Economically, the levelized cost of energy ($LCOE$) is treated as the leading economic parameter that can reflect the economic feasibility of any energy production system. The current study considers a system lifetime of 20 years, with a currency inflation rate of 5%. The $LCOE$ for the TSR system recorded 0.225 $/kW h, which is 30% lower than that of the bare system (the $LCOE$ for the bare system recorded 0.318 $/kW h); see Fig. 13 and Table 4. A critical consideration concerning the energy production of WECS is the output degradation across time. Herein, we consider a reduction of 25% of the rated power after 30 years of operation, as reported in [34]. The aging of the energy production for the bare and the modified system is plotted in Fig. 14. In this study, we consider the payback period as the output of the savings by considering the electricity tariff from the grid as a reference.

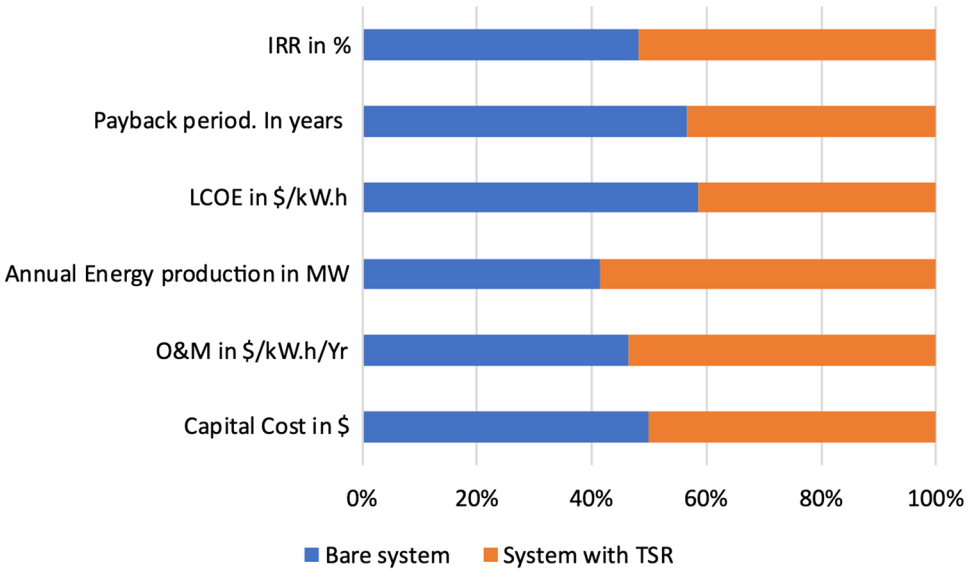

Fig. 13 Economic outputs with and without the TSR system

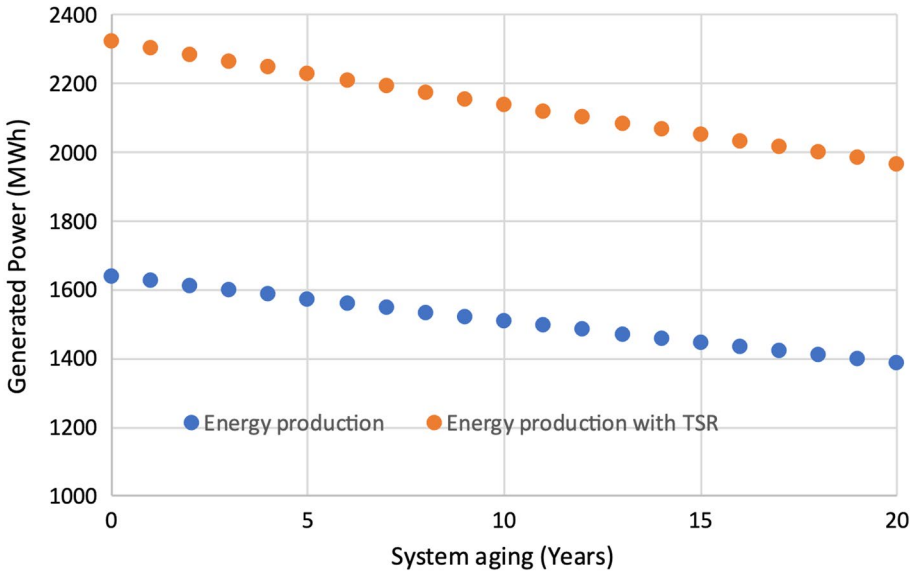

Fig. 14 System aging energy production with and without TSR system

For the environmental aspects, while referring to the density of electric vehicles, as demonstrated in Fig. 4, the total daily EVs approaching the station can reach 179 EVs. Considering the grid as the benchmark for charging the station, which is operated by natural gas, the required energy results in approximately 171.75 metric tons of CO_2 emissions annually. A critical consideration related to manufacturing energy technologies is the construction energy and carbon intensities [35]. In the case of land-based wind turbines, both the construction energy and carbon intensities are the lowest compared to other energy generation technology alternatives, scoring an average of 424 kg/kW of CO_2 and 6697 MJ/kW, respectively [35]. In other words, for a 3.5 MW wind turbine to be constructed, approximately 1860 tons of CO_2 will be released into the environment. Consequently, the carbon footprint of the wind turbine is approximately equivalent to half the emissions produced from the station under grid operation during the 20 years lifetime. An additional selling edge for the current study is related to replacing gasoline vehicles with EVs. For a typical scenario of gasoline vehicles, the average annual emissions are approximately 4.6 metric tons of CO_2 per vehicle [10]. Accordingly, the proposed 179 vehicles' total annual emissions are equivalent to 300,541 metric tons of CO_2.

Finally, a significant aspect related to any renewable energy resource in general, and WECS in specific, is the system relatability. The WECS reliability is a concrete function in the wind speed dynamics, the higher the extreme wind speed the lower the system life spam. Fortunately, the allocation of our proposed system, as previously highlighted

in section two, is associated with low-wind dynamics location, which positively impact the system reliability. Moreover, an added O&M cost is mainly dedicated to service the consequences of implementing TSR algorithm, which can elongate the system lifetime. Over, and above, in this study we consider the worst-case prediction for a wind turbine aging, only 20 years, where reported literature indicates up to 30 years wind turbine operation under appropriate maintenance [34].

6 Conclusion

This study investigates the impact of implementing a tip speed ratio algorithm on a wind turbine-PMSG system that provides energy to an EV charging station in El Sherouk City, located in New Cairo, Egypt. The simulation of the system is conducted using MATLAB/Simulink software, considering the energy demand of EVs in the Egyptian automotive market and the wind characteristics specific to Cairo, Egypt. The results of the system simulation, optimized by the TSR MPPT algorithm, demonstrate a significant increase in energy yield by 41.68%. This increase in energy yield, achieved through the implementation of MPPT algorithms, not only helps reduce the system size but also lowers the overall system cost or allows for an increase in the capacity of EVs. Furthermore, the Levelized Cost of Energy analysis reveals a 30% reduction, indicating improved financial viability with a shortened payback period and a higher rate of return on investment. Considering the environmental aspect, during the construction of a 3.5 MW wind turbine, it is estimated that around 1860 tons of CO_2 will be released into the environment. As a result, the carbon footprint associated with the wind turbine is approximately equivalent to half of the emissions produced by the station under grid operation over its 20-year lifetime. This highlights the importance of considering the environmental impact not only during the operation phase but also during the construction phase of renewable energy projects. Finally, a significant advantage of the current study is its focus on replacing gasoline vehicles with EVs. In a typical scenario involving gasoline vehicles, each vehicle emits an average of approximately 4.6 metric tons of CO_2 annually. Taking this into account, the total annual emissions from the proposed 179 vehicles would amount to approximately 300,541 metric tons of CO_2. This stark comparison underscores the potential for reducing carbon emissions by transitioning to EVs and further emphasizes the importance of promoting sustainable transportation options.

Author contributions Conceptualization, SA; methodology, SA; software, AK and SA validation, AK and SA; formal analysis, AK and SA investigation, A. K and SA; resources, A. K and SA; data curation, AK and SA writing—original draft preparation, AK and SA; writing—review and editing, SA, GE, and HG; visualization KA, and SA; supervision, SA, GE, and HG; project administration, SA, GE, and HG. All authors have read and agreed to the published version of the manuscript.

Funding The authors would like to acknowledge the support and contribution of the Centre for Emerging Learning Technologies (CELT) at the British University in Egypt (BUE).

Data availability The datasets generated during and/or analyzed during the current study are available from the corresponding author upon reasonable request.

Code availability Not applicable for that section.

Declarations

Ethics approval consent to participate Not applicable.

Consent for publication Not applicable.

Competing interests The authors declare no conflict of interest.

References

1. Harvey JA, Tougeron K, Gols R, et al. Scientists' warning on climate change and insects. Ecol Monogr. 2023;93(1): e1553.
2. Eckardt NA, Ainsworth EA, Bahuguna RN, et al. Climate change challenges, plant science solutions. Plant Cell. 2023;35(1):24.
3. Bulkeley H, Newell P. Governing climate change. Milton Park: Taylor & Francis; 2023.
4. Auffhammer M. Climate adaptive response estimation: short and long run impacts of climate change on residential electricity and natural gas consumption. J Environ Econ Manag. 2022;114: 102669.
5. Raihan A, Begum RA, Nizam M, Said M, Pereira JJ. Dynamic impacts of energy use, agricultural land expansion, and deforestation on CO2 emissions in Malaysia. Environ Ecol Stat. 2022;29(3):477.
6. Lukin E, Krajnović A, Bosna J. Sustainability strategies and achieving SDGs: a comparative analysis of leading companies in the automotive industry. Sustainability. 2022;14(7):4000.
7. Nunes A, Woodley L, Rossetti P. Re-thinking procurement incentives for electric vehicles to achieve net-zero emissions. Nat Sustain. 2022;5(6):527.
8. Ledna C, Muratori M, Yip A, Jadun P, Hoehne C. National Renewable Energy Lab. (NREL), Golden, CO (United States). 2022.
9. Axsen J, Hardman S, Jenn A. What do we know about zero-emission vehicle mandates? Environ Sci Technol. 2022;56(12):7553.
10. Xia X, Li P, Xia Z, Wu R, Cheng Y. Life cycle carbon footprint of electric vehicles in different countries: a review. Sep Purif Technol. 2022;122063.
11. Powell S, Cezar GV, Min L, Azevedo IM, Rajagopal R. Charging infrastructure access and operation to reduce the grid impacts of deep electric vehicle adoption. Nat Energy. 2022;7(10):932.
12. Jenn A, Highleyman J. Distribution grid impacts of electric vehicles: a California case study. IScience. 2022;25(1): 103686.
13. Ismail AA, Mbungu NT, Elnady A, Bansal RC, Hamid A-K, AlShabi M. Impact of electric vehicles on smart grid and future predictions: a survey. Int J Model Simul. 2022. https://doi.org/10.1080/02286203.2022.2148180.
14. Biya T, Sindhu M. 2019 3rd International conference on Electronics, Communication and Aerospace Technology (ICECA) IEEE, 2019.
15. Elkasrawy M, Makeen P, Abdellatif SO, Ghali HA. Optimizing electric vehicles station performance using AI-based decision maker algorithm. In: Emerging topics in artificial intelligence 2020, vol. 11469, pp. 68–75.
16. Elkasrawy M, Hassan A, Abdellatif S, Ebrahim G, Ghali H. Prototyping design and optimization of smart electric vehicles/stations system using ANN. Int J Electr Comput Eng Syst. 2022;13(6):485.
17. Elkasrawy M, Abdellatif SO, Ebrahim GA, Ghali HA. Real-time optimization in electric vehicle stations using artificial neural networks. Electr Eng. 2023;105(1):79.
18. Makeen P, Memon S, Elkasrawy M, Abdullatif SO, Ghali HA. Smart green charging scheme of centralized electric vehicle stations. Int J Green Energy. 2021;19(5):490–8.
19. Elkasrawy M, Makeen P, Abdullatif SO, Memon S, Ghali HA. Investigating the utility of water cycle optimization and non-linear programming techniques in electric vehicle stations smart planning. IETE J Res. 2022;1–13.
20. Shankareppagol LM, Hampannavar S, Doadamani SN. 2018 3rd International Conference for Convergence in Technology (I2CT) IEEE, 2018.
21. Kumar D, Chatterjee K. A review of conventional and advanced MPPT algorithms for wind energy systems. Renew Sustain Energy Rev. 2016;55:957.
22. Bahgat A, Helwa N, Ahmad G, El Shenawy E. Maximum power point traking controller for PV systems using neural networks. Renew Energy. 2005;30(8):1257.
23. Mousa HH, Youssef A-R, Mohamed EE. State of the art perturb and observe MPPT algorithms based wind energy conversion systems: a technology review. Int J Electr Power Energy Syst. 2021;126: 106598.
24. Dbaghi Y, Farhat S, Mediouni M, Essakhi H, Elmoudden A. Indirect power control of DFIG based on wind turbine operating in MPPT using backstepping approach. Int J Electr Comput Eng. 2021;11(3):1951.
25. Ram JP, Rajasekar N, Miyatake M. Design and overview of maximum power point tracking techniques in wind and solar photovoltaic systems: a review. Renew Sustain Energy Rev. 2017;73:1138.
26. Cai Y, Li M, Wang T, Wang X, Razik H. An output power interval control strategy based on pseudo-tip-speed ratio and adaptive genetic algorithm for variable-pitch tidal stream turbine. J Mar Sci Eng. 2022;10(9):1197.
27. Babu PS, Sundarabalan C, Balasundar C, Krishnan TS. Fuzzy logic based optimal tip speed ratio MPPT controller for grid connected WECS. Mater Today: Proc. 2021;45:2544.
28. Hamid B, Hussain I, Iqbal SJ, Singh B, Das S, Kumar N. Optimal MPPT and BES control for grid-tied DFIG-based wind energy conversion system. IEEE Trans Ind Appl. 2022;58(6):7966.
29. Ghandi A, Sergey P. Global CO2 impacts of light-duty electric vehicles. Transportation Research Part D: Transport and Environment 87(2020):102524.
30. Glahn HR, David PR. The new digital forecast database of the National Weather Service. Bull Am Meteorol Soc 2003;84.2:195–202.
31. Reyes V, Rodríguez JJ, Carranza O, Ortega R. 2015 IEEE 24th International Symposium on Industrial Electronics (ISIE) IEEE, 2015.
32. Diallo M, Youssef S, Gualous H, Camara M, Dakyo B. 2014 16th International Power Electronics and Motion Control Conference and Exposition IEEE, 2014.
33. Mokhtari Y, Rekioua D. High performance of maximum power point tracking using ant colony algorithm in wind turbine. Renew Energy. 2018;126:1055.
34. Byrne R, Astolfi D, Castellani F, Hewitt NJ. A study of wind turbine performance decline with age through operation data analysis. Energies. 2020;13(8):2086.
35. Morini AA, Ribeiro MJ, Hotza D. Carbon footprint and embodied energy of a wind turbine blade—a case study. Int J Life Cycle Assess. 2021;26:1177.